

The Crystal Structure of TiCu_2P and Its Relationship to the Structure of Mn_3As

WILDER CARRILLO-CABRERA

Institute of Chemistry, University of Uppsala, Box 531, S-751 21 Uppsala, Sweden

The crystal structure of TiCu_2P has been determined from single-crystal X-ray diffractometer data. The structure has been refined to an $R(F^2)$ value of 0.077 without excluding any reflections. The space group is $I4_1/amd$ (No. 141). The tetragonal unit cell, of dimensions $a=3.5164(2)$ Å and $c=33.574(3)$ Å, contains eight formula units. TiCu_2P contains structural units which are found in other transition-metal phosphides and arsenides. The TiCu_2P structure type, which can be derived from the Mn_3As structure by a glide operation, belongs to the Cu_2Sb structure family. It is shown that NdTe_3 and Mn_3As , whose crystal structures have been described in different space groups, are geometrically equivalent (*i.e.* NdTe_3 is an antitype to Mn_3As).

In the course of a study of the Ti–Cu–P alloy system, a ternary phase with the approximate composition TiCu_2P was found.¹ This paper presents a complete single-crystal X-ray determination of the structure of TiCu_2P , showing that the composition and the space group assignment given in Ref. 1 are correct. However, the structure is closely related to the Cu_2Sb family rather than TiAl_3 , as suggested earlier.¹

EXPERIMENTAL

Preparation. Titanium (Koch-Light Laboratories, Colnbrook, England, claimed purity 99.999 %) was arc-melted together with material of the composition $\text{CuP}_{0.15}$ (prepared by the sealed silica tube method¹ at 800 °C), in an atmosphere of purified argon. The solidified melt (approx. 2.5 g, nominal composition $\text{Ti}_{0.10}\text{Cu}_{0.78}\text{P}_{0.12}$) thus prepared was found to contain the TiP ,² Cu_3P (low temperature form³) and Cu phases. Subsequently the ternary sample was heat-treated at 800 °C for 84 h and plate-

like crystals and aggregates of TiCu_2P were then formed (TiP was also present in the copper matrix). After dissolving the matrix in nitric acid, a very thin plate-like crystal was selected for collecting the X-ray intensity data. It was limited by the $\{100\}$ and $\{001\}$ faces and its dimensions were approximately $56 \times 48 \times 3$ μm (its smallest extension being along the c -axis). Larger crystals were obtained by longer heating periods at temperatures between 800 and 950 °C, but the quality of the crystals was poorer.

Significant variations of the unit cell dimensions of TiCu_2P were observed, indicating a range of homogeneity. The unit cell volume varied from $414.64(2)$ Å³ (Ref. 1), for a specimen in an alloy ($\text{Ti}_{0.07}\text{Cu}_{0.78}\text{P}_{0.15}$; 900 °C, 11d) with nominal Ti/P = 0.47, to $414.89(4)$ Å³ for a specimen in an alloy ($\text{Ti}_{0.33}\text{Cu}_{0.33}\text{P}_{0.33}$; 900 °C, 14d) with nominal Ti/P = 1.00. The latter volume value is slightly smaller than that in Table 1 ($415.14(6)$ Å³), which was measured on a specimen in a more copper rich alloy with nominal Ti/P = 0.83, that was however, heat-treated at 800 °C.

X-Ray diffraction measurements and data reduction. The cell dimensions were determined using a Guinier-Hägg focusing camera with $\text{CuK}\alpha_1$ radiation ($\lambda=1.540598$ Å) and semiconductor grade silicon ($a=5.431065$ Å)⁴ as calibration standard, and least-squares refined using the local program CELNE.⁵ The equipment and single-crystal X-ray data collection procedure have been described previously.⁶ Intensities of all the reflections were measured up to $2\theta=25^\circ$ to check the space group conditions and absorption (as well as possible extinction) correction. For $25^\circ < 2\theta < 100^\circ$ only reflections with $h, k,$ and l positive and $h+k+l=2n$ were recorded. The instrumental stability and crystal setting were checked by remeasuring three test reflections. Totally 1766 reflections were measured. After checking the conditions of the space group, reflections that should be systematically absent were

deleted [all of them had $I < 3\sigma(I)$]. In order to correct for absorption and extinction effects only the reflections having identical indices (*e.g.* test reflections) were averaged. The X-ray data were thus reduced to 1082 reflections. The intensities were corrected for Lorentz and polarization effects.

After applying absorption and extinction corrections, equivalent reflections were averaged, which reduced the material to 538 non-equivalent reflections. Correction for absorption was applied using the Gaussian grid method and a linear absorption coefficient of 252 cm^{-1} (calculated with the mass absorption coefficients given in Ref. 7). The minimum and maximum transmission factors obtained were 0.373 and 0.907. Extinction effects were taken care of by a method devised by Coppens and Hamilton.⁸

The numerical calculations were performed using IBM 1800 and NORD 100 computers. Crystallographic programs used for the structure analysis are described in Ref. 5.

STRUCTURE DETERMINATION AND REFINEMENT

Inspection of Weissenberg films, taken with crystals rotating about the *a* and *c* axes, indicated and *I*-centred tetragonal cell. Furthermore, they showed systematic absences for *hk0* and *hhl* reflections corresponding to the $I4_1/amd$ (No. 141) space group. A closer look at the diffractometer data revealed additional conditions for the *hkl* reflections: $2h + l = 2n + 1$ or $4n$, which indicates 8(*e*), 4(*b*) and 4(*a*) as possible atom sites. These special conditions are also valid for the non-centrosymmetric space group $I4_1md$ with the atoms at the 4(*a*) site. The centrosymmetric alternative was chosen and finally confirmed in the refinement.

The very strong (0 0 16) reflection and the long *c*-axis indicated that the atoms must be essentially confined to planes $\sim c/16$ apart. Moreover, the very weak (0 0 8) reflection indicated that the sets of atomic layers which are $\sim c/8$ apart scatter almost equally. The unit cell volume and the approximate composition TiCu_2P suggested a unit cell content of 32 atoms (16 copper, 8 titanium and 8 phosphorus). These facts, coupled with interatomic distance considerations and the possible similarity to other known structures were utilized to construct trial models of the structure.

A reasonable model of the structure could be constructed with all the atoms at 8(*e*) sites. A series of refinements on *F* and F^2 was then started. A

full-matrix least-squares program⁵ and complex neutral-atoms scattering factors were used.⁷ Extinction effects were discernible and an isotropic correction was applied.⁸ The following 10 parameters were initially refined: one scale factor, one isotropic extinction parameter, four positional parameters and four isotropic temperature factors. The refinement, based on F^2 converged to an $R(F^2)$ value of 0.094 [$R_w(F^2) = 0.093$].

Incorporation of anisotropic temperature factors for three atoms (three further parameters were refined) resulted in a significant drop in the *R*-values: the refinement on F^2 with anisotropic temperature factors for Cu(1), Cu(2) and P (atoms in Ti site were found to vibrate isotropically) converged to $R(F^2) = 0.088$ and $R_w(F^2) = 0.088$ for the whole material (1082 reflections). The standard deviation of an observation of unit weight⁹ was $S = 1.08$. A ΔR plot¹⁰ gave a least-squares line with a slope of 1.04 and an intercept of -0.05 (on the expected ΔR axis) in the interval $|R| < 4.0$. The largest extinction correction was 32%. An internal consistency factor (defined in Ref. 6) for symmetry related reflections (126 reflections, of which 20 were non-equivalent) with $2\theta < 25^\circ$ decreased from 3.90% (after absorption correction only) to 3.06%, after extinction correction. The agreement indices used in the text have been defined elsewhere.¹¹ The function minimized in the refinement on F^2 was $\Sigma w(F_o^2 - F_c^2)^2$. Weights were assigned to the reflections according to the formula $w^{-1} = \sigma_c^2(F_o^2) + (pF_o^2)^2$, where $\sigma_c^2(F_o^2)$ is based on counting statistics and the empirical factor *p*, which modifies *w* to obtain a satisfactory weight analysis, was set to 0.020.

When occupancies were allowed to vary, no significant deviations from full occupancy were found. The composition of the crystal investigated, selected from a copper-rich alloy, is thus TiCu_2P .

A final refinement on F^2 using averaged extinction-corrected data (538 reflections) gave $R(F^2) = 0.077$ and $R_w(F^2) = 0.059$. At this stage a final Fourier difference synthesis was calculated. It exhibited no positive or negative peaks exceeding 6% of a phosphorus maximum in the corresponding F_o synthesis.

A list of observed and calculated structure factors can be obtained on request from the Institute of Chemistry, University of Uppsala, Uppsala, Sweden. Final structure data are presented in Table 1. Corresponding interatomic distances are given in Table 2.

Table 1. Final structural data^a for TiCu₂P (from refinement based on F^2), including anisotropic thermal parameters^b U_{ij} ($\times 10^4$) \AA^2 . Standard deviations are given in parentheses.

Space group: $I4_1/amd$ (No. 141)
 Unit cell dimensions: $a = 3.5164(2) \text{\AA}$, $c = 33.574(3) \text{\AA}$;
 $V = 415.14(6) \text{\AA}^3$; $Z = 8$.
 Calculated density: 6.59 g/cm^3

Atom	z	U_{11}	U_{33}
Cu(1)	0.09753(3)	63(3)	94(4)
Cu(2)	0.40468(3)	66(3)	85(3)
P	0.29612(5)	36(5)	60(6)
Ti	0.22198(3)	^c	

^aAll the atoms lie in the special position 8(e) and the origin at $4m2$. ^bThe anisotropic temperature factor is of the form: $\exp[-2\pi^2 U_{11}(h^2 + k^2)a^{*2} - 2\pi^2 U_{33}l^2c^{*2}]$; $U_{22} = U_{11}$, $U_{12} = U_{13} = U_{23} = 0$. ^c $U_{\text{iso}} = 58(2) \times 10^{-4} \text{\AA}^2$.

DESCRIPTION AND DISCUSSION OF THE TiCu₂P STRUCTURE

A projection of the structure along the a -axis is illustrated in Fig. 1. The projection of the atomic environment of Cu(1) [being identical to that of Cu(2)] and the corresponding one for Ti are outlined in Fig. 1. It should be mentioned that neighbours which are situated at distances 22% larger than the corresponding atomic radius sum are not considered to belong to the near environment of the central atom. The Goldschmidt metal radius (12 C.N.) and the tetrahedral covalent radius of phosphorus have been used to calculate the radius

Table 2. Interatomic distances in TiCu₂P. The table shows all M–P and P–P distances less than 3.65 \AA and M–M distances less than 4.20 \AA . Standard deviations within parentheses.

Cu(1)–2P	2.464(1)	Cu(2)–2P	2.412(1)
–4Cu(2)	2.488(0)	–4Cu(1)	2.488(0)
–2Cu(1)	2.548(1)	–2Cu(1)	2.602(1)
–2Cu(2)	2.602(1)	–2Cu(2)	2.658(1)
–2Ti	2.922(1)	–2Ti	2.863(1)
–4Cu(1)	3.516(0)	–4Cu(2)	3.516(0)
–Ti	4.178(1)	–P	3.645(2)
P–2Cu(2)	2.412(1)	Ti–P	2.489(2)
–2Cu(1)	2.464(1)	–4P	2.560(1)
–Ti	2.489(2)	–2Cu(2)	2.863(1)
–4Ti	2.560(1)	–2Cu(1)	2.922(1)
–P	3.516(0)	–4Ti	3.118(1)
–Cu(2)	3.645(2)	–4Ti	3.516(0)
		–Cu(1)	4.178(1)

sums.^{12,13} In Table 2, a gap in the list of interatomic distances indicates this borderline. The copper and titanium atoms have thus 12 and 17 nearest neighbours. High coordination numbers (= number of nearest neighbours) for the larger atoms (Ti) as in this metal-rich compound (with radius ratios $r_P/r_{\text{Ti}} = 0.76$, $r_P/r_{\text{Cu}} = 0.86$, $r_{\text{Cu}}/r_{\text{Ti}} = 0.88$) occur in other transition-metal silicides, phosphides and arsenides as well (e.g. Ti_7P_4 (Nb_7P_4) and related compounds¹⁴). It should be emphasized that the coordination of copper in the structure of pure copper metal (face-centred cubic, A1 type) is a

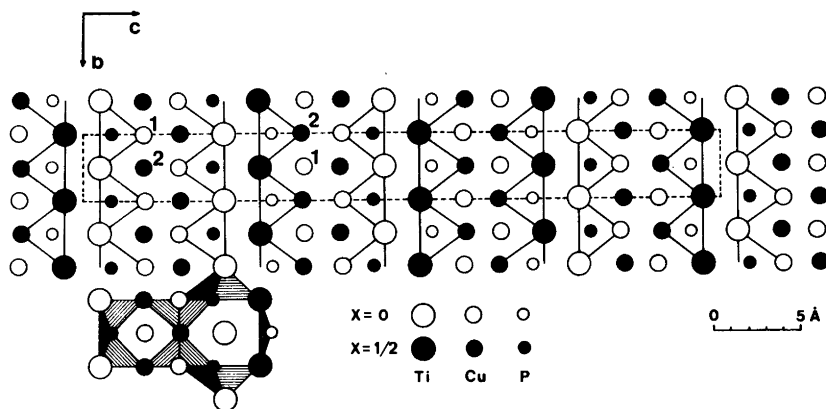


Fig. 1. Projection of the structure of TiCu₂P as viewed along the a -axis.

regular cubo-octahedron, which is distorted in TiCu_2P due to the replacement of four copper atoms by two titaniums and two phosphorus atoms.

Each phosphorus atom has nine metal neighbours. Eight of them are located at the corners of a somewhat distorted Archimedean or square-antiprism (the square formed by the four copper atoms has a side $1/\sqrt{2}$ shorter than that formed by the four titaniums) and the remaining titanium atom is situated outside the larger square face of the antiprism. The atomic environment of phosphorus can also be described as a tricapped trigonal prism with three atoms (2Cu+1Ti) outside the quadrilateral faces of the prism (this environment occurs frequently for *p*-elements in compounds with transition metals¹⁵). Only the triangular faces of the prism or square-antiprism are indicated in the projection of TiCu_2P in Fig. 1.

From Table 2 it is evident that only the Ti–P distances along the *c*-axis and the Cu–Cu distances along $[110]$ direction are shorter than the radius sum of 2.55 and 2.56 Å, respectively. All the Cu–P, Cu–Ti and Ti–Ti distances are larger than the corresponding radius sum (2.38, 2.73 and 2.90 Å, respectively).

The structure of TiCu_2P can also be described as a stacking of 16 atomic layers. Eight of these are practically planar and formed by copper atoms only (Cu layers) and the other eight are puckered, with

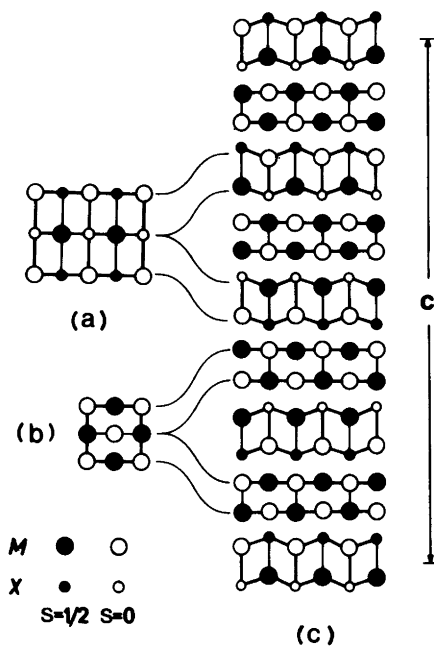


Fig. 2. Comparison of the projection of the structures of (a) NaCl (B1 type) along the $[110]$ direction and (b) Cu (face-centred cubic, A1 type) along the *a*-axis with that of (c) TiCu_2P along the *a*-axis. M=metal, X=non-metal and *s* is the fractional height along the direction of projection.

Table 3. Crystallographic data for Mn_3As .

Space group <i>Pmmn</i> (Ref. 18)					Space group <i>Bmmb</i> (this work)				
Atom	Position	<i>x</i>	<i>y</i>	<i>z</i>	Atom	Position	<i>x</i>	<i>y</i>	<i>z</i>
Mn(1)	2a	0	0	0.1935	Mn(1,4)	4c	0	1/4	0.0565
Mn(4)	2b	0	1/2	0.3065	Mn(2,5)	4c	0	1/4	0.4435
Mn(2)	2a	0	0	−0.1935	Mn(3,6)	4c	0	1/4	0.6845
Mn(5)	2b	0	1/2	−0.3065	As(1,2)	4c	0	1/4	0.841
Mn(3)	2a	0	0	−0.4345					
Mn(6)	2b	0	1/2	−0.0655					
As(1)	2a	0	0	0.409					
As(2)	2b	0	1/2	0.091					

an equal number of titanium and phosphorus atoms (Ti–P layers). By examination of the form of packing of the layers, fragments of the face-centred cubic (Cu, A1 type) and NaCl (B1 type, ZrP phase¹⁶ also adopts this type) structures can be identified. The width of the Cu-like slices is half the unit cell length of the Cu structure and the NaCl-like fragments are layers of distorted half-cells of the NaCl type as demonstrated in Fig. 2. The two types of fragments are packed together, alternating along the c -axis of TiCu_2P .

The TiCu_2P structure constitutes a new structure type. Considering the composition and the metallic lustre of its crystals, the compound is likely to be metallic.

The main features of the structure of TiCu_2P presented in Figs. 1 and 2c, reveal a striking resemblance to Fe_2As ¹⁷ (C38, Cu_2Sb type¹⁷) and related structures: Mn_3As ,¹⁸ NdTe_3 ,¹⁹ Nd_2Te_5 ²⁰ and La_2Sb ²¹ (Ti_2Bi type²²). Since the relationship of the latter structures to the C38 type has been established in the earlier descriptions of the structures, we restrict this part of the discussion to describe the relationship between TiCu_2P and Mn_3As structures only. It may first be mentioned that the structure of Mn_3As is in fact the antitype to that of NdTe_3 , although they have been described in different space groups. In the structure of Mn_3As ($Pm\bar{m}n$, Ref. 18) the atoms are either at $2(a)$ or $2(b)$ (see left part of Table 3). By first adding $3/4$ to all y -coordinates and then subtracting $1/4$ from all z -coordinates (*i.e.* shifting the origin to $0, -3/4, 1/4$), it appears that two positions [one $2(a)$ and one $2(b)$] in $Pm\bar{m}n$ correspond to only one position, $4(c)$, in $Bm\bar{m}b$ (identical with $Cm\bar{c}m$, No. 63). Thus it seems more appropriate to describe the Mn_3As structure in the space group $Bm\bar{m}b$ (see right part of Table 3).

The structures of Mn_3As (anti- NdTe_3) and TiCu_2P are compared in Fig. 3, as viewed along the a -axis. The figure shows how the position of six common subunits (denoted by C_1) changes in the two structures. This subunit consists of one unit cell of the Fe_2As structure. In Fig. 3, it can also be distinguished that TiCu_2P and Mn_3As contain another common subunit (denoted by C_2) which coincides with one unit cell of the Mn_3As structure. Each cell represents one *slab* (formed by interconnected Fe_2As or Mn_3As cells). The TiCu_2P structure can thus be derived from the Mn_3As structure through a glide operation. In this manner, these structures can be regarded as different stackings of *slabs* of Fe_2As (C_1 type) or Mn_3As (C_2 type)

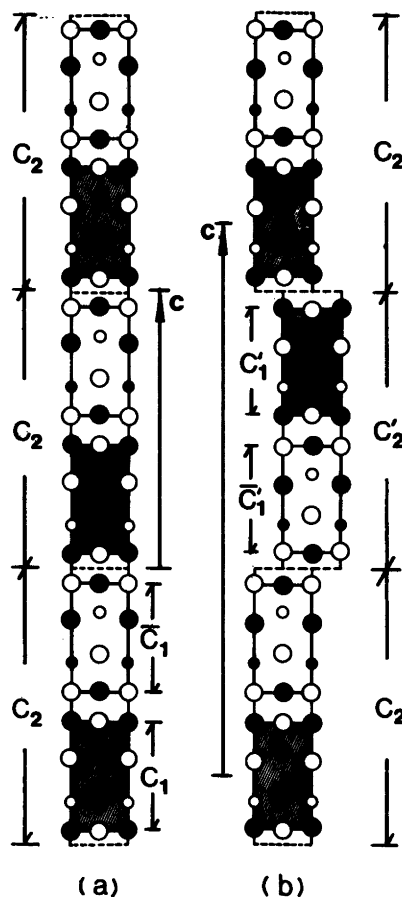


Fig. 3. Structural relationships between (a) Mn_3As (anti NdTe_3 , $Bm\bar{m}b$ setting) and (b) TiCu_2P structures, as viewed along the a -axis. The notations are consistent with those given for Fig. 2.

unit cells. In Table 4, the respective stacking sequence and the slip between adjacent *slabs* (C_1 or C_2) in the structures of Fe_2As , Mn_3As and TiCu_2P are given.

There are other structures, for instance Mo_8P_5 and Cr_3C_2 ,^{23,24} which contain other kinds of structural fragments common to Fe_2As (C38) structure type. The structural fragments in common are built up of atomic layers, which are perpendicular to the a (or b) directions in Fe_2As .

Acknowledgements. The author is indebted to Professor S. Rundqvist and Docent T. Lundström for valuable discussions and for their criticism of

Table 4. Stacking sequence of C_1 -slabs (or C_2 -slabs) of Fe_2As (or Mn_3As) unit cells in the Fe_2As , Mn_3As and $TiCu_2P$ structures.

Structure	Stacking sequence ^a	Glide between slabs		
		Slab pairs	Slip magnit.	Slip direct.
Fe_2As	$C_1C_1\dots$	C_1C_1	0	—
Mn_3As	$C_1\bar{C}_1C_1\bar{C}_1\dots$	$C_1\bar{C}_1$	$a/2$	[100]
	or $C_2C_2\dots$	C_2C_2	0	—
$TiCu_2P$	$C_1\bar{C}_1C_1'\bar{C}_1'C_1\bar{C}_1C_1'\bar{C}_1'\dots$	$C_1\bar{C}_1$ or $C_1'\bar{C}_1'$	$a/2$	[100]
	or $C_2C_2'C_2C_2'\dots$	\bar{C}_1C_1 or C_2C_2'	$b/2$ $(a+b)/2$	[010] [110]

^a C_1 = slab perpendicular to the c -axis of Fe_2As with a width equal to c_{Fe_2As} . \bar{C}_1, C_1' or C_1 = slabs displaced relative to C_1 perpendicular to the stacking (c) direction. C_2 = slab perpendicular to the c -axis of Mn_3As with a width equal to c_{Mn_3As} . C_2' = slab displaced relative to C_2 perpendicular to the stacking (c) direction.

the manuscript. The financial support of the Swedish Natural Science Research Council is gratefully acknowledged.

REFERENCES

- Carrillo-Cabrera, W. and Lundström, T. *Acta Chem. Scand. A* 33 (1979) 401.
- Snell, P.-O. *Acta Chem. Scand.* 21 (1967) 1773.
- Olofsson, O. *Acta Chem. Scand.* 26 (1972) 2777.
- Deslattes, R. D. and Henis, A. *Phys. Rev. Lett.* 31 (1973) 972.
- Lundgren, J.-O., Ed., *Crystallographic Computer Programs*, Institute of Chemistry, University of Uppsala, Uppsala 1975. UUIC-B13-04-02.
- Carrillo-Cabrera, W. and Lundström, T. *Acta Chem. Scand. A* 34 (1980) 415.
- International Tables for X-Ray Crystallography*, Kynoch Press, Birmingham 1974, Vol. 4.
- Coppens, P. and Hamilton, W. C. *Acta Crystallogr. A* 26 (1970) 71.
- Abrahams, S. C. *Acta Crystallogr. A* 25 (1969) 165.
- Abrahams, S. C. and Keve, E. T. *Acta Crystallogr.* 27 (1971) 157.
- Carrillo-Cabrera, W. and Lundström, T. *Acta Chem. Scand. A* 35 (1981) 545.
- Laves, F. *Theory of Alloy Phases*, Am. Soc. Metals, Cleveland, Ohio 1956.
- Pauling, L. *Nature of the Chemical Bond*, 3rd Ed., University Press, Ithaca, New York 1960.
- Carrillo-Cabrera, W. *Acta Chem. Scand. A* 36 (1982) 563.
- Aronsson, B., Lundström, T. and Rundqvist, S. *Borides, Silicides and Phosphides*, Methuen, London 1965.
- Irani, K. S. and Gingerich, K. A. *J. Phys. Chem. Solids* 24 (1963) 1153.
- Elander, M., Hägg, G. and Westgren, A. *Ark. Kemi Mineral. Geol. B* 12 (1936) 1.
- Nowotny, H., Funk, R. and Pesl, J. *Monatsh. Chem.* 82 (1951) 513.
- Nordling, B. K. and Steinfink, H. *Inorg. Chem.* 5 (1966) 1488.
- Pardo, M.-P. and Flahaut, J. *Bull. Soc. Chim. Fr.* (1967) 3658.
- Stassen, W. N., Sato, M. and Calvert, L. D. *Acta Crystallogr. B* 26 (1970) 1534.
- Auer-Welsbach, H., Nowotny, H. and Kohl, A. *Monatsh. Chem.* 89 (1958) 154.
- Johnsson, T. *Acta Chem. Scand.* 26 (1972) 365.
- Rundqvist, S. and Runnsjö, G. *Acta Chem. Scand.* 23 (1969) 1191.

Received April 27, 1982.